



Published by Fusion Energy Division, Oak Ridge National Laboratory
Building 5700 P.O. Box 2008 Oak Ridge, TN 37831-6169, USA

Editor: James A. Rome
E-Mail: jar@ornl.gov

Issue 113
Phone (865) 482-5643

February 2008

On the Web at <http://www.ornl.gov/sci/fed/stelnews>

High ion temperature plasma production in LHD

Ion temperature T_i has been successfully increased in the Large Helical Device (LHD) in Toki, Japan. In FY 2006 (the 10th experimental campaign), T_i exceeded 5 keV at an average plasma density n_e of $1.2 \times 10^{19} \text{m}^{-3}$, and it has exceeded 6 keV at $n_e \sim 2 \times 10^{19} \text{m}^{-3}$ in FY 2007 (the 11th campaign). These achievements have demonstrated the capability of high- T_i plasma confinement in helical devices, which leads towards a helical fusion reactor. In this report, we summarize the highlights of high- T_i plasma production experiments in FY 2006. Further progress in FY 2007 will be reported somewhere in the near future.

The Setup for Ion Heating Experiments in LHD

The most powerful heating system in LHD is negative-ion-based neutral beam injection (NBI), provided by three tangential injectors with nominal hydrogen injection energy of 180 keV [1]. The total injection power from tangential NBI has reached about 14 MW. One injector (#2) has the opposite injection direction to the other two injectors (#1 and #3). A low-energy positive NBI system (#4) with perpendicular injection became operational in FY 2005, and it achieved 40-keV 7-MW injection in FY 2006.

To demonstrate high- T_i plasma confinement capability in LHD, high-Z (such as Ne and Ar) plasmas with low ion density (in the range of 10^{17}m^{-3}) were previously used as targets when only tangential NBIs were available, to effectively increase the absorption power per ion. With this approach T_i of about 13.5 keV was successfully demonstrated [2]. This successful proof-of-principle experiment for high- T_i plasma confinement has led to the installation/power increase of a low-energy NBI system to directly increase the ion heating power. As noted earlier, beam #4 is perpendicularly injected, enabling charge-exchange recombination spectroscopy (CXS) measurement with a toroidal line of sight for radial profiles of T_i and toroidal rotation velocity (V_t), even in cases in which impurity content (utilized for measurement) has a hollow density profile. A schematic view of the NBI configuration and CXS

system is provided in Ref. [3]. Information on the T_i and V_t profiles enhances the physics understanding of the confinement characteristics of helical plasmas.

Heating in the ion cyclotron range of frequency (ICRF) [4] can also be utilized because the target plasmas for high- T_i experiments in LHD are now the lighter ion species, such as hydrogen and/or helium. A total ion cyclotron heating (ICH) power of about 2 MW (38.47 MHz) was injected through four antennas using the minority-ion heating mode.

In addition, electron cyclotron heating (ECH) has been recognized as an effective way to improve ion confinement in the core region through the appearance of the electron-root radial electric field (E_r) [2]. This effect was clearly recognized at $n_e \sim 0.3 \times 10^{19} \text{m}^{-3}$ in high-Z plasmas. Since the target density for the high- T_i hydrogen plasma production experiments described in this report is above 10^{19}m^{-3} , clear effects of ECH on ion energy confinement have not yet been observed, although an increase

In this issue . . .

High ion temperature plasma production in LHD

Ion temperature (T_i) has been successfully increased in the Large Helical Device (LHD) in Toki, Japan. In FY 2006 (the 10th experimental campaign), T_i exceeded 5 keV at an average plasma density (n_e) of $1.2 \times 10^{19} \text{m}^{-3}$, and it has exceeded 6 keV at $n_e \sim 2 \times 10^{19} \text{m}^{-3}$ in FY 2007 (the 11th campaign). These achievements have demonstrated the capability of high- T_i plasma confinement in helical devices, which leads towards a helical fusion reactor. In this report, we summarize the highlights of high- T_i plasma production experiments in FY 2006. Further progress achieved in FY 2007 will be reported in the near future. 1

Changes in the ORNL Stellarator Program

James Lyon retired at the end of January. His role is being assumed by Jeffrey Harris. 5

All opinions expressed herein are those of the authors and should not be reproduced, quoted in publications, or used as a reference without the author's consent.

Oak Ridge National Laboratory is managed by UT-Battelle, LLC, for the U.S. Department of Energy.

in the T_i gradient (in discharges with T_i in the range of 1 keV) at the core region was observed.

These heating methods were applied in reduced helical ripple magnetic configurations with R_{ax} in the range 3.575–3.65 m and magnetic field strength (B) of 2.7–2.85 T. Here R_{ax} is the vacuum magnetic axis position. To condition the wall for high- T_i experiments He-glow discharge cleaning is usually performed during the previous night, and titanium gettering is done the morning of the operational day to reduce the high- Z impurity influx and to make the density easier to control.

The Heating Scenario for High- T_i Experiments in LHD

ECH is applied for plasma start-up. It is important to grasp the ion heating capability of injector #4 since its injection power P_{inj} has been increased. The core T_i values measured by the crystal spectrometer [5] (with only injector #4 in operation) are summarized in Fig. 1, where the core T_i is plotted as a function of ion-heating power P_i (roughly estimated as 80% of the deposition power) normalized by ion density. Increasing P_i/n_i provides a steady increase in core T_i as shown by data clusters for $P_{inj} = 1.4$ (green squares), 2.2 (green circles), and ~ 5 MW, exceeding 2 keV with only the injector #4. For $P_{inj} \sim 5$ MW, the heating capability was examined in detail to elucidate a favorable heating scenario. One is the scenario of “ECH \rightarrow high-energy NBI \rightarrow low-energy NBI” (blue triangles) and the other is “ECH \rightarrow low-energy NBI” (red circles). The latter scenario gives higher T_i in general, indicating that low-energy NBI injected just after the ECH phase is useful to “prepare” base high- T_i plasmas. Although the reason for this finding has not yet been fully understood, prevention of hollow density profiles (typically seen with tangential NBI) and/or keeping the electron temperature T_e low (high-energy NBI primarily heats electrons) might be plausible explanations.

ICH is also anticipated to increase T_i in hydrogen/helium plasmas. Density scan experiments were performed by using a minority ion heating scenario (helium as minority ion) with a resonance region close to the magnetic axis (38.47 MHz). The injection power reached 2 MW. Figure 2 shows T_i measured by crystal spectroscopy as a function of line-averaged density for several heating scenarios. The results with only NBI (both high- and low-energy beams) are shown by black circles, those with high-energy beams and ICH by blue circles, and those with ICH only by red circles. It is difficult to measure the core T_i for cases with significantly hollow impurity profiles (crystal spectroscopy measurement use the Ar line), which often occur as T_i becomes higher (the so-called impurity hole) [3]. Thus, T_i values in this figure (especially at higher T_i) may indicate the values, for example, at mid-radius where the impurity line intensity is adequate for the measurement.

Thus, the actual T_i in the core region seems to be higher than plotted in Fig. 2. However, the general response of T_i to heating scenario can be seen from this figure. The effective increase of T_i with ICH (for example, red circles) is observed at $n_e < 1 \times 10^{19} \text{ m}^{-3}$. Compared to this, NBI effectively heats the hydrogen ions when $n_e > 1 \times 10^{19} \text{ m}^{-3}$, as indicated by open circles. This figure clearly indicates that the superposition of ICH for high- T_i plasma production should be effective when $n_e \sim 1 \times 10^{19} \text{ m}^{-3}$.

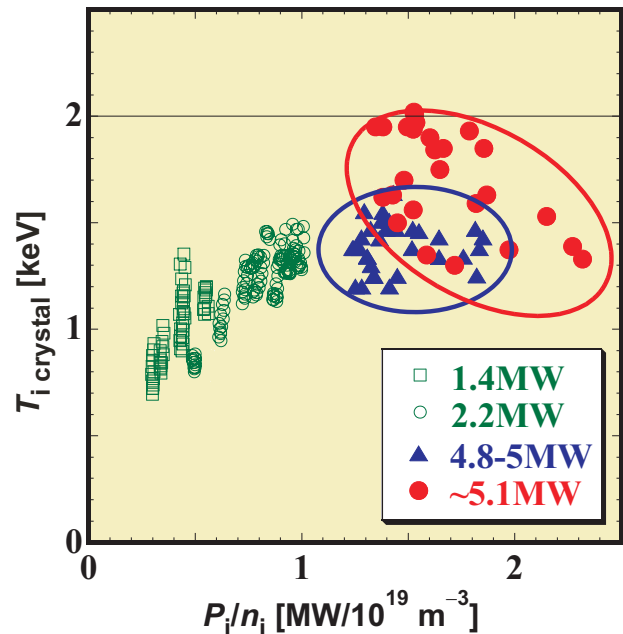


Fig. 1. Core T_i (with the injector #4 only) as a function of ion heating power normalized by ion density for cases with $P_{inj} = 1.4$ (green squares), 2.2 (green circles), and ~ 5 MW. In the case of $P_{inj} = 5$ MW, data for two heating scenarios are shown; one is “ECH \rightarrow high-energy NBI \rightarrow low-energy NBI” (blue triangles) and the other is “ECH \rightarrow low-energy NBI” (red circles).

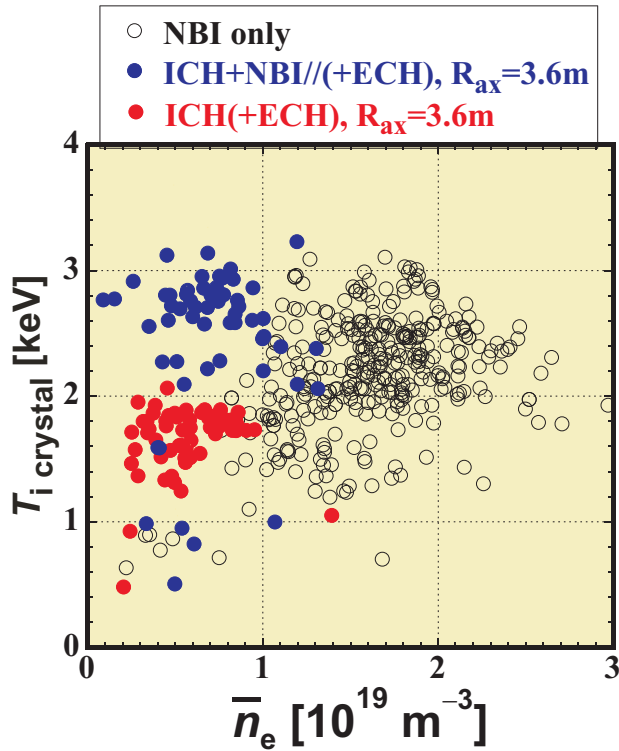


Fig. 2. T_i as a function of line-averaged density for several heating scenarios. The results with only NBI (both high- and low-energy beams) are shown by black circles, those with high-energy NBI and ICH by blue circles, and those with ICH only by red circles.

High- T_i Hydrogen Plasma Production in LHD

Based on the above-mentioned constructive information for high- T_i plasma production, high- T_i hydrogen plasmas (exceeding 5 keV) were successfully demonstrated in LHD.

Figure 3 shows the details of a 5.2-keV discharge at $n_e \sim 1.2 \times 10^{19} \text{ m}^{-3}$, where the following results are shown: (a) the heating scenario, (b) T_i (measured by CXS), (c) T_e (measured by Thomson scattering) and (d) V_t (induced by CXS) profiles. The magnetic configuration is characterized by $R_{ax} = 3.575 \text{ m}$ with $B = -2.769 \text{ T}$ (B direction reversed), which makes injectors #1 and #3 into co-injectors and #2 into a counter-injector. Injector #4 consists of four ion sources with the two independently-operatable power supply systems (4A and 4B). This flexibility was utilized to modulate one of power supplies (in this case, 4B) for injection at a 100 ms interval to obtain the background signals, as seen at the bottom of Fig. 3(a). Injector #4 was used from 0.5 s (just after ECH-off) for 1 s, with superposition of injectors #1–#3 from 0.9 s onward.

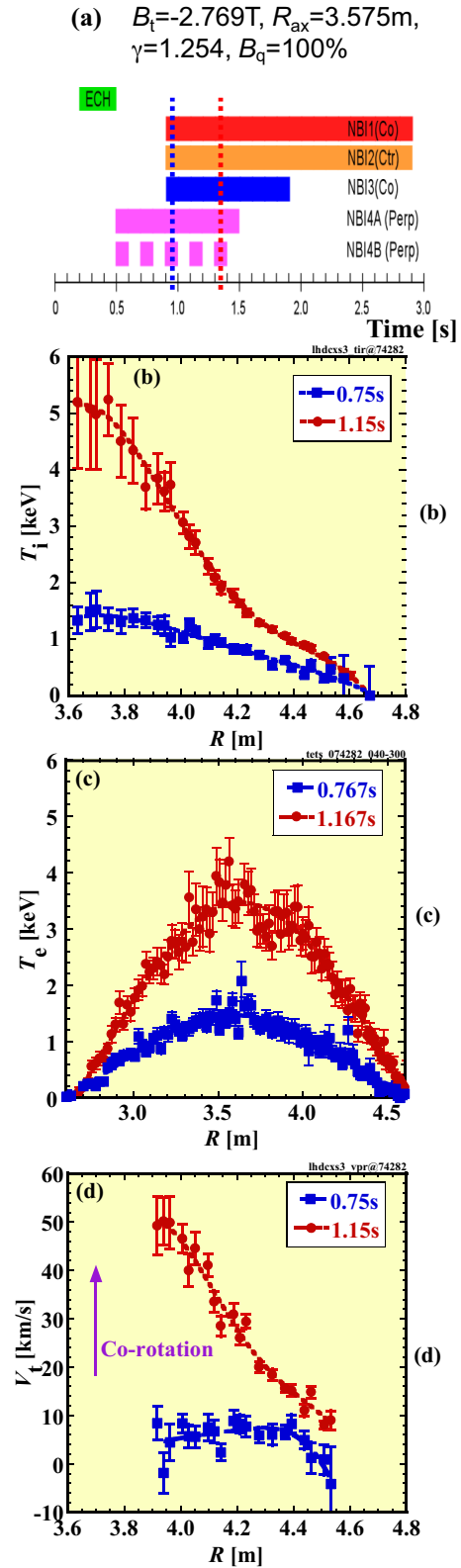


Fig. 3. (a) The heating scenario, (b) T_i , (c) T_e , and (d) V_t profiles of a 5.2-keV discharge heated only by NBI.

ICH was not applied in this example. At $t = 0.75$ s, with injector #4 alone, T_i reaches about 1.6 keV with comparable T_e . The density profile at this time is peaked due to the particle fueling from injector #4 [6], and V_t is rather small (less than 10 km/s). Once the injectors #1–#3 are injected with a superposition of injector #4, T_i increases and reaches 5.2 keV at the core region with an apparent change of the gradient around $R \sim 4.3$ m. This change of the T_i gradient indicates that ion energy confinement is improved at the inner region. In this high- T_i phase, T_i exceeds T_e [~ 3.5 keV at the core region, as seen in Fig. 3(c)]. The density profile tends to become flat to hollow, which is a typical trend for plasmas heated by high-energy NBI in LHD. V_t is also largely enhanced in the co-direction in accordance to the predominance of co-injected beams. V_t at the very core region becomes difficult to be deduced due to the lack of line intensity for the measurement. However, at least as much as 50 km/s of V_t (about 7% of the thermal velocity of hydrogen ions at 5.2 keV) is observed.

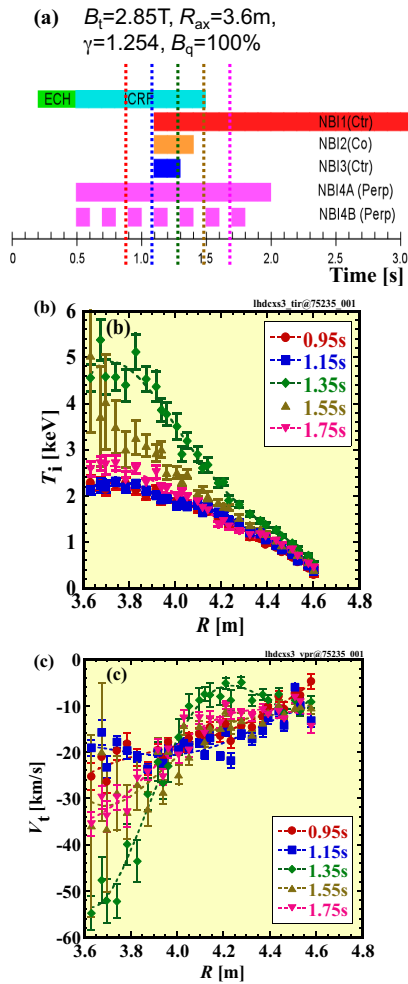


Fig. 4. (a) The heating scenario, (b) T_i and (c) V_t profiles of about 5 keV discharge heated by NBI and ICH.

Another example of a high- T_i discharge with ICH at a slightly larger density, about $1.6 \times 10^{19} \text{ m}^{-3}$, is shown in Fig. 4: (a) the heating scenario, (b) T_i , and (c) V_t profiles. The magnetic configuration is $R_{ax} = 3.6$ m with $B = 2.85$ T (normal direction of B) making counter-injection dominant (injectors #1 and #3 are counter injecting). In this case, ICH (~ 2 MW) is superimposed on beam #4 just after ECH-off and followed by the further superposition of beams #1–#3 from 1.1 s. T_i exceeds 2 keV during the application of beam #4 and ICH, and further increases up to about 5 keV at 200–300 ms after the injection of beams #1–#3. Note that T_i does not increase at $t = 1.15$ s (just after the injection of beams #1–#3). V_t increases in the counter direction at the time of the maximum T_i . Note also that core T_e increases from about 2 keV at $t = 0.95$ s to 3.5 keV at $t = 1.35$ s, and then falls to 3 keV at $t = 1.75$ s. Thus, $T_i > T_e$ is again the case at the time of the maximum T_i .

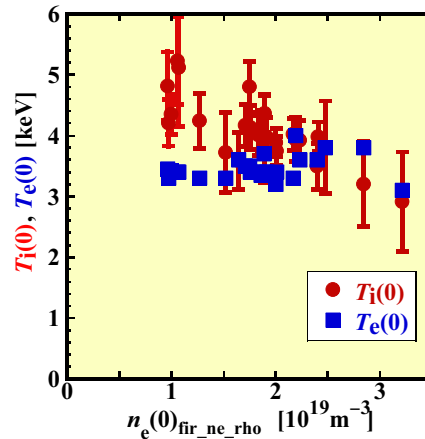


Fig. 5. T_i and T_e as a function of core n_e in the density scan experiment.

Density scan experiments were also performed in majority hydrogen plasmas with the heating scenario shown in Fig. 3(a). The results are summarized in Fig. 5, where core T_i and T_e are plotted as a function of the core electron density deduced from the CO₂ laser-pumped far infrared (FIR) measurement [7]. It is clear that T_i exceeds T_e at the lower density regime and then tends to become comparable to T_e as the density is increased. T_i exceeds 3 keV even at $n_e \sim 3.2 \times 10^{19} \text{ m}^{-3}$. This figure summarizes the achieved extension of high- T_i regime in the FY 2006 experiments in LHD.

Summary

High-ion-temperature (exceeding 5 keV) hydrogen plasmas were successfully produced in the FY 2006 experiments in LHD. The injection power of the low-energy NBI was upgraded to 6–7 MW, which effectively enhanced the direct ion heating power. This beam line is also utilized as

the observation beam for CXS with a toroidal line of sight. It has provided profile information about the toroidal rotation as well as the ion temperature. ICH is also applied in superposition to NBI, to extend the density regime of plasma with ion temperature of about 5 keV.

Transport analyses (with a special focus on ripple-transport suppression in the low collisional regime with $T_i/T_e > 1$) reported at the APS-DPP meeting in 2007 by the author (to appear in *Physics of Plasmas*), are not repeated here.

It should be noted that as of January 2008, the FY 2007 experiments are still going on, and further increases in T_i (to >6 keV) has been achieved at $n_e \sim 2 \times 10^{19} \text{ m}^{-3}$ with more detailed and sophisticated utilization of NBI power to further enhance ion confinement. This further progress will be reported in the near future.

Masayuki Yokoyama for the LHD Experimental Group
National Institute for Fusion Science
Toki, Japan
E-mail: yokoyama@LHD.nifs.ac.jp

References

- [1] O. Kaneko et al., Nucl. Fusion **43** (2003) 692.
- [2] Y. Takeiri et al., Nucl. Fusion **47** (2007) 1078.
- [3] M. Yoshinuma, *Stellarator News*, Issue 111, Oct. 2007.
- [4] K. Saito et al., Nucl. Fusion **41** (2001) 1021.
- [5] S. Morita et al., Rev. Sci. Instrum. **74** (2003) 2375.
- [6] K. Nagaoka et al., submitted to Plasma and Fusion Res. (2007), based on presentation at the 17th International Toki Conference, 16th International Stellarator/Heliotron Workshop, Oct. 2007.
- [7] K. Kawahata et al., Rev. Sci. Instrum. **70** (1999) 707.

Changes in the ORNL Stellarator Program

The responsibility for the stellarator program at Oak Ridge National Laboratory (ORNL) has been transferred from James Lyon to Jeffrey Harris. Dr. Lyon served in that role since the mid-1980s during his nearly 44 years in the fusion program at ORNL. He retired at the end of January.

Jeff Harris will become NCSX Deputy Project Manager and QPS Project Manager and is already responsible for ORNL stellarator collaborations (with Japan, Europe, and Australia). Dr. Harris has worked at ORNL from 1981 to 1997 and returned to ORNL in 2005. In between he was Professor and Head of the H1 Helicac project at the Australian National University. Jeff has worked on experiments in Russia, France, Japan, and Spain.

ORNL's Rajesh Maingi will remain as the person responsible for preparing for the ORNL research program on NCSX, in addition to his responsibilities in the NSTX program. In addition, Don Hillis and Stan Milora will be strengthening the ORNL stellarator program by taking a more active role.